

Article

Impact of Power on Uneven Development: Evaluating Built-Up Area Changes in Chengdu Based on NPP-VIIRS Images (2015–2019)

Long Liu ¹, Zhichao Li ², Xinyi Fu ³, Xuan Liu ^{3,*} , Zehao Li ⁴ and Wenfeng Zheng ⁵ 

¹ School of Political Science and Public Administration, East China University of Political Science and Law, Shanghai 200042, China; 3024@ecupl.edu.cn

² School of International and Public Affairs, Shanghai Jiao Tong University, Shanghai 200240, China; lizhichao@ecupl.edu.cn

³ School of Public Affairs and Administration, University of Electronic Science and Technology of China, Chengdu 611731, China; 202021160324@std.uestc.edu.cn

⁴ School of Information Engineering, China University of Geosciences, Beijing 100083, China; 11007192127@cugb.edu.cn

⁵ School of Automation, University of Electronic Science and Technology of China, Chengdu 611731, China; winfirms@uestc.edu.cn

* Correspondence: liuxuan@uestc.edu.cn

Abstract: In the context of uneven development studies of China, urban built-up area changes are the index of the impact of power, as the local government is the only party that is able to acquire agricultural land and convert it to construction urban land. Existing studies generally use statistical data to describe the built-up area changes and struggle to meet the requirement of an updated and inexpensive monitoring of uneven development, especially for western cities with tight budgets. Open access NPP-VIIRS (Suomi National Polar-orbiting Partnership Visible Infrared Imaging Radiometer Suite), NDVI (Normalized Difference Vegetation Index), and nighttime LST (Land Surface Temperature) data ranging from 2015 to 2019 were analyzed with a stratified SVM (Support Vector Machine) method in this study to track urban built-up area changes in Chengdu, one of the biggest cities in Western China. The SDE (Standard Deviation Ellipse) and Moran's *I* were then applied to evaluate the spatial variations of the built-up area changes. It was revealed that the spatial evolution of built-up area change in Chengdu over the period 2015–2019 demonstrated a “northwest-southeast” spatial expansion pattern, and the change distance in the center of gravity in 2018 and 2019 was greater than that from 2015 to 2017, which reflected the faster uneven development in 2018 and 2019 in Chengdu. The results were verified with finer resolution Landsat-8 OLI images; the high OA (all larger than 92%) and KAPPA (all larger than 0.6) values showed the accuracy of the method. The methodology proposed in this study offers a practical way for cities with tight budgets to monitor uneven development, and this study suggests a further adaption using higher-resolution remote sensing images and field experiments.

Keywords: uneven developments; urban urban built-up area; Chengdu; NPP-VIIRS



Citation: Liu, L.; Li, Z.; Fu, X.; Liu, X.; Li, Z.; Zheng, W. Impact of Power on Uneven Development: Evaluating Built-Up Area Changes in Chengdu Based on NPP-VIIRS Images (2015–2019). *Land* **2022**, *11*, 489. <https://doi.org/10.3390/land11040489>

Academic Editors: Pere Serra and Marta Sapena

Received: 13 February 2022

Accepted: 23 March 2022

Published: 28 March 2022

Publisher's Note: MDPI stays neutral with regard to jurisdictional claims in published maps and institutional affiliations.



Copyright: © 2022 by the authors. Licensee MDPI, Basel, Switzerland. This article is an open access article distributed under the terms and conditions of the Creative Commons Attribution (CC BY) license (<https://creativecommons.org/licenses/by/4.0/>).

1. Introduction

Uneven development is understood as a basic geographical hallmark of the capitalist mode of production: capital produces unevenness on purpose to generate cycles of accumulation [1,2]. The practices to produce and exploit space to the maximum extent cause a remarkable scale of uneven development, especially in some developing countries, such as China [3]. According to the theory of ‘production of space’, uneven development in one place is both a process and result of the uneven geographical base and developmental context, which are shaped by capital, power, and class [4]. Monitoring the factors that

structure the developmental context becomes important to understand and prevent uneven development [5].

Based on China's urban development context, Yeung et al. (2019) suggested using the built-up (constructed urban land) area as the index of power. This is because the local government is the only buyer of agricultural land and the only seller of construction land in one Chinese city, and is often the main driving force for extending and expanding the constructed urban land [6]. Yeung et al. (2019) also applied the indexes system to analyze the uneven development in Jiangsu Province, for which the information of the built-up area is provided in statistical data. However, the statistics data applied in Jiangsu, a rich coastal province, could hardly be obtained and renewed on time in western cities with tight budgets in China [6]. A new method for the updated and inexpensive monitoring of built-up areas is, therefore, needed.

Recently, remote sensing information, such as nighttime stable light (NTL) data, has become widely acknowledged as a new resource to objectively reflect the changes in urban development and the related issues. However, there are two main deficiencies that degrade the accuracy of urban land extracted from NTL data. First, heavy cloud in bad weather constrains the precision of the NTL data [7], which needs to be processed in advance. Second, the overflow effects in the urban core areas limit the accuracy identity of the urban built-up area [8], which needs to be adjusted by other data sources. In response to the gaps above, this paper designed a method to extract the built-up area of Chengdu, a big city in Western China with open access NTL data. In detail, the Suomi National Polar-orbiting Partnership Visible Infrared Imaging Radiometer Suite (NPP-VIIRS) NTL data, the Moderate-Resolution Imaging Spectroradiometer (MODIS) Normalized Difference Vegetation Index (NDVI) data, and the MODIS nighttime Land Surface Temperature (LST) data were utilized, and a stratified support vector machine (SVM) algorithm was applied to gain a better evaluation of the built-up area. Additionally, the refined results of the built-up area were analyzed with Standard Deviation Ellipse (SDE) to track the dynamic change in the built-up area. Finally, the global and local Moran's *I* analysis was employed to explore the geographic correlation within Chengdu from 2015 to 2019.

2. Literature Reveiw

As a promising remote sensing data source for urban studies, NTL data are an indirect manifestation of human activities and have been widely used in the study of built-up area change, environmental problems, socioeconomic development, and many other socio-economic issues. For example, the NTL data can be widely employed in many city-level or country-level socio-economic affairs, including monitoring urban industrial energy consumption [9], detecting the economic development in major cities in the Democratic People's Republic of Korea (DPRK) [10], and estimating the population trends in prefecture-level cities in China from 1992 to 2018 [11]. In terms of urbanization, the NTL data can not only evaluate the built-up area change in the major urban agglomerations in China [8], such as the Yangtze River Delta Urban Agglomeration [12] and the Guangdong-Hong Kong-Macao Greater Bay Area [13], but can also precisely measure the urban shrinkage at the county-level city in China [14]. In summary, there are two main kinds of NTL data sources that contain NTL data for different years globally, namely, the Defense Meteorological Satellite Program's Operational Line Scan System (DMSP/OLS) NTL data and the NPP-VIIRS NTL data. Since the DMSP/OLS NTL data are available online earlier than NPP-VIIRS NTL data, some studies have already employed DMSP/OLS NTL data to study the built-up area change. For example, Ma et al. (2015) [15] delineated that NTL brightness correlated with rural-urban gradients in the process of built-up area change using DMSP/OLS NTL data. The dynamics of built-up area change in China were described with DMSP/OLS NTL data [16]. Together with remote sensing images, DMSP/OLS NTL data also helped examine built-up area change in Chengdu [17].

However, the saturation issue due to the digital number value of DMSP/OLS NTL data ranging from 0 to 63, limit the performance of DMSP/OSL NTL data in urban built-up

areas [18]. Although some remote sensing image or NDVI data were applied to reduce the mistakes of DMSP/OLI NTL data [19], it is still reported that the impact from the variations in the atmospheric condition may severely impact the effectiveness of the application of DMSP/OLS in the study of built-up area change [20].

As a new generation of night-time satellite products, NPP-VIIRS NTL data enabled the daily, monthly, and annual data collection ranging from 2012 to the present. After the NPP-VIIRS NTL data were made available online, a few researchers conducted comparative studies between these two NTL data sources [21–23]; their results proved that the performance of NPP-VIIRS NTL data was outweighed by the DMSP/OLS data in terms of better calibration, a wider dynamic range and the ability to identify thermal sources. For example, the NPP-VIIRS NTL data are highly effective in calibration and validation, which could detect night-time lights spanning from 75° N to 65° S with radiation from $3 \text{ nW}\cdot\text{cm}^{-2}\cdot\text{sr}^{-1}$ to $0.02 \text{ W}\cdot\text{cm}^{-2}\cdot\text{sr}^{-1}$ [24]. Therefore, the application of NPP-VIIRS NTL data to study and analyze urban development has drawn much more attention recently.

In addition to the common heavy clouds issue, the overflow effects issue also constrains the accuracy of NPP-VIIRS NTL data in urban areas [8]. Therefore, increasing research has employed other remote sensing data sources as auxiliary data to improve the performance of NPP-VIIRS NTL data in urban scenarios. For example, the NDVI data and the nighttime LST data from the MODIS platform, which can effectively distinguish the urban and rural areas, are often employed to improve the accuracy of NPP-VIIRS NTL data in the urban study area [8,16,25], and their results clearly demonstrate the effects of these two auxiliary data sources. Therefore, in this research, we also employed the NDVI data and the nighttime LST data to improve the accuracy of the NPP-VIIRS NTL data in Chengdu.

In terms of urban-related studies, there are three main methods to extract urban built-up areas based on NTL data, namely, the thresholding, the index, and the supervised classification method, as one of the most popular supervised classification methods, stratified SVM, can achieve better performance than the thresholding and the index method [24]. In addition, according to related research [16,26,27], the extraction results of the stratified SVM method demonstrated more accuracy and reliability than other methods. Furthermore, as one of the non-parametric machine learning methods [28], SVM can not only solve the nonlinear and high dimensional data classification problem [25], but can also achieve better performance based on a few training samples [26]. Considering the regional diversity, the urban development level varies in different regions, the stratified SVM can classify unknown pixels at different levels within a specific region precisely by employing a regional-specific stratified method [27]. Therefore, considering the complex situation between the boundary of the urban and non-urban areas, the stratified SVM method was employed to extract the urban built-up area based on NPP-VIIRS NTL data, NDVI data, and nighttime LST data, following related research [26,27].

In addition, there is not enough research to address the city-level socioeconomic affairs and businesses in Western China, e.g., whether these western cities have expanded due to the economic growth in recent years in China, or whether these western cities have shrunk due to people moving to the eastern cities in China. However, it is crucial for decision-makers to understand the temporal-spatial pattern of western cities in China in a timely and precise manner.

Therefore, this paper extracted the urban built-up area of Chengdu over the period 2015–2019 from the NPP-VIIRS NTL data, the NDVI data, and the nighttime LST data using the stratified SVM method, coupled with the SDE, to analyze the dynamic characteristics of the temporal-spatial variations [29,30]. In addition, the global and local Moran's I indexes of the economic variation were calculated based on statistical data in the Statistical Year Book from 2015 to 2019 [31].

3. Methodology

3.1. Study Area

In this research, the study area chosen was the city of Chengdu (see Figure 1). Chengdu is located in southwestern China; its geographic coordinates are $30^{\circ}05'–31^{\circ}26'$ north latitude and $102^{\circ}54'–104^{\circ}53'$ east longitude.

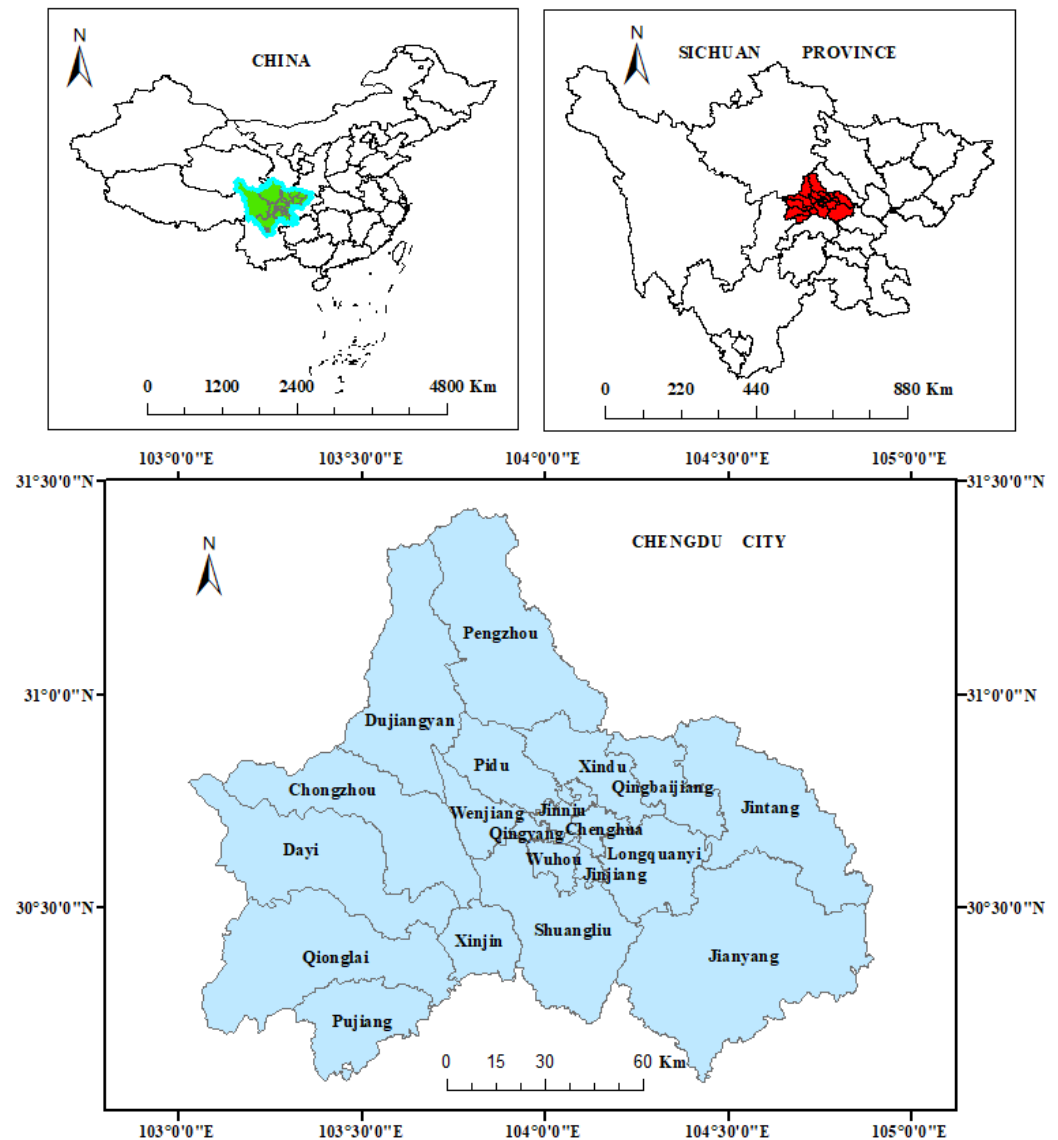


Figure 1. Location of Chengdu.

It includes 11 urban districts (Jinjiang, Wuhou, Chenghua, Jinniu, Qingyang, Xindu, Longquanyi, Qingbaijiang, Pidu, Wenjiang and Shuangliu), and 9 towns (Pengzhou, Dujiangyan, Chongzhou, Qionglai, Jianyang, Dayi, Pujiang, Xinjin and Jintang). Chengdu is the capital city of Sichuan province and plays a vital and indispensable role in Western China in terms of politics, economy, and culture. Having a better understanding of the expansion patterns of Chengdu is conducive to a rational allocation of resources, and a better design for scientific blueprints of common development. According to the 2020 National Census of China, Chengdu's population was over 20 million people, covering the landmass of $14,335 \text{ km}^2$, which is one of the largest urban areas in the whole of China. The Gross Domestic Product (GDP) of Chengdu in 2019 was more than CNY 1534 billion, an increase of 8% compared to the previous last year, ranking in the top 10 in the whole

country. As the gateway to Western China and as the major and most important area of Development Planning of Chengdu and Chongqing Urban Agglomeration released by the central government, it is the responsibility of Chengdu to give full play to the functions of strategic support and exemplary radiation in order to coordinate the socioeconomic development regionally and also of West China. According to the Chengdu City Master Plan from 2016 to 2035, the leading role Chengdu should take is to become an open-oriented economic highland along the Belt and Road Initiative and hub city internationally. This led to dense investment in the south and east parts of Chengdu. A new method is needed for the long-term and close monitoring of uneven development.

3.2. Data Sources

In this paper, the NPP-VIIRS NTL data, with version Annual VNL V2 [7], were downloaded from the Earth Observation Group website (<https://eogdata.mines.edu/products/vnl/> (accessed on 30 September 2021)), which was launched by the National Aeronautics and Space Administration (NASA), the National Oceanic and Atmospheric Administration (NOAA) and the U.S. Air Force in 2011; their Suomi-National Polar-orbiting Partnership consists of 22 imaging and radiometric bands and covers wavelengths ranging from 0.41 to 12.5 microns, providing the sensor data records, including clouds and sea surface temperature. Their NPP-VIIRS not only performed very well in calibration and validation, but could also detect the NTL data spanning from 75° N to 65° S with the radiation from $3 \text{ nW}\cdot\text{cm}^{-2}\cdot\text{sr}^{-1}$ to $0.02 \text{ W}\cdot\text{cm}^{-2}\cdot\text{sr}^{-1}$ [17]. In addition, the DNB (Day/Night Band) is a component of the VIIRS Instrument onboard Suomi NPP, which makes it possible for satellite observation at night in the visible spectrum. Therefore, we extracted their NPP-VIIRS NTL data of Chengdu from 2015 to 2019, which were in 15 arc-second geographic grids, equal to 500 m spatial resolution.

In addition, the nighttime LST data were collected from the NASA website (<https://ladsweb.modaps.eosdis.nasa.gov/> (accessed on 30 September 2021)); the 1000 m spatial resolution 8-day composite nighttime LST data of MODIS (MOD11A2-level3) were employed to distinguish the urban area from other non-urban areas. Following the Maximum Value Composite (MVC) method [16,26,27], the annual nighttime LST images were produced in Chengdu from 2015 to 2019. Furthermore, the MODIS 16-day composite NDVI data were also obtained from the NASA website, which was at a 250 m spatial resolution. The MVC method was also employed to obtain an annual NDVI image. We resampled the NPP-VIIRS NTL data, the nighttime LST data, and NDVI data to unify 1000 m spatial resolution for further calculation.

Other auxiliary data include the yearly MODIS Land Cover Type product (MCD12Q1), the Landsat-8 Operational Land Imager (OLI) data, and the socio-economic census data and administrative boundary data. The MCD12Q1 data were collected from the NASA website (<https://ladsweb.modaps.eosdis.nasa.gov/> (accessed on 30 September 2021)), which had a 500m spatial resolution [32]; in addition, the accuracy of the MODIS Land Cover Type dataset product was evaluated in China [33]. The high-quality and fine-resolution Landsat images from Landsat-8 OLI data were employed to evaluate the urban built-up area extraction results, which were downloaded from the Geospatial Data Cloud website (<https://www.gscloud.cn/> (accessed on 30 September 2021)), within the Chengdu area (path/row:129-130/38-39). The socioeconomic census data we employed to analyze the variation were downloaded from the Statistical Database of Economic and Social Development by the National Knowledge infrastructure of China (<https://data.cnki.net/> (accessed on 30 September 2021)). The administrative boundaries were downloaded from the National Geomatics Center of China in GIS files format (<http://www.ngcc.cn/ngcc/> (accessed on 30 September 2021)).

The three main data sources, namely, the NPP-VIIRS NTL data, the MODIS NDVI data, and the MODIS nighttime LST data, are listed in Figure 2. Considering the overflow effect of the NPP-VIIRS NTL data, the MODIS NDVI data and the MODIS nighttime LST data can help the NPP-VIIRS NTL data to distinguish the urban and non-urban areas more

accurately. Therefore, a combination of these three different types of data sources can enable a better understanding of the temporal-spatial characteristics of the urban built-up area change.

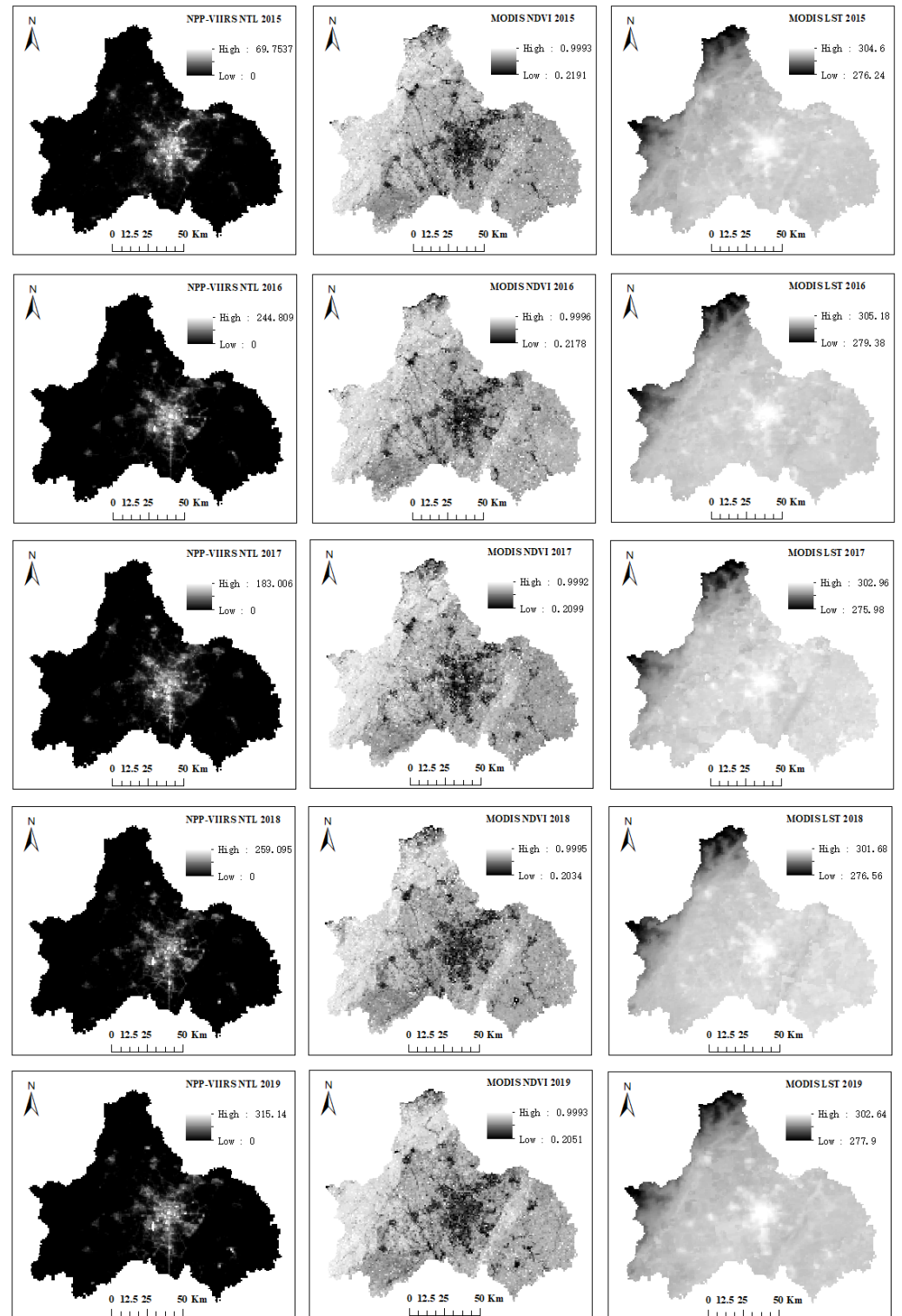


Figure 2. The data of three main data sources in Chengdu from 2015 to 2019.

3.3. Data Processing

3.3.1. Workflow

The main process in this research can be divided into three main steps, as it is illustrated in Figure 3. First, we extracted the urban built-up area based on the stratified SVM method and then evaluated the accuracy of extraction results based on the Landsat-8 OLI data and MODIS Land Cover data. Second, the SDE analysis method was employed to analyze the built-up area change pattern of Chengdu from 2015 to 2019. Third, Moran's index analysis was employed to discuss the geographic correlation of urban built-up areas over the five years.

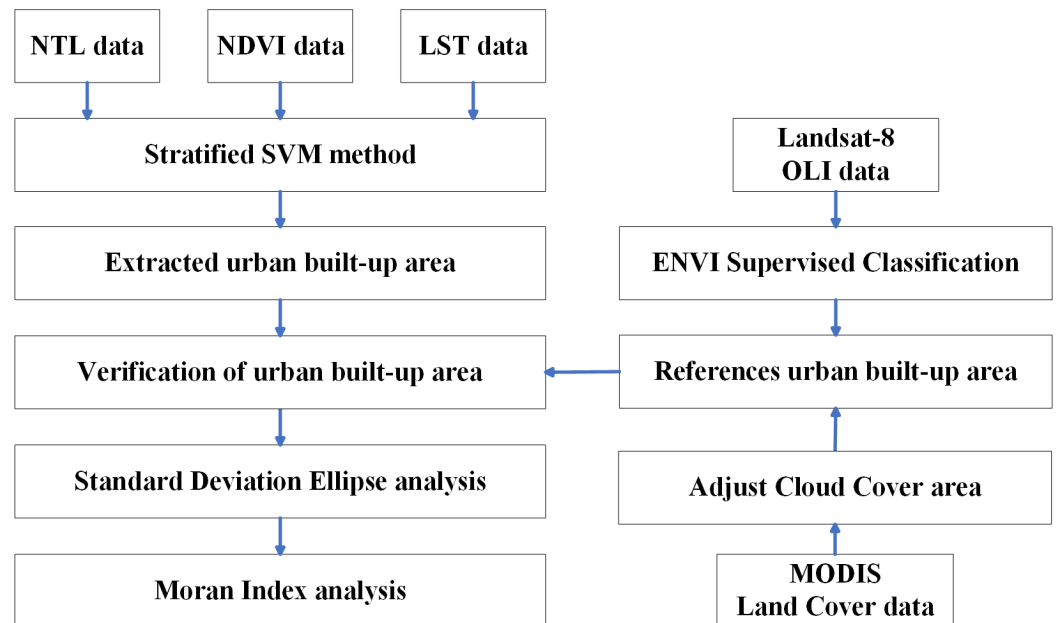


Figure 3. The flowchart of the proposed research.

3.3.2. Pre-Processing

We resampled the NPP-VIIRS NTL data at 1000 m spatial resolution after downloading the annual data; then, the administrative regionalization mask was employed to extract the nighttime lights images of Chengdu from 2015 to 2019. The annual NDVI and LST data were obtained based on the MVC method following similar research [19]. All three main data were projected to uniform Albers projection with 1000 m resolution.

3.3.3. Stratified SVM-Based Urban Built-Up Areas Extraction

In terms of the urban extraction method [26,27], the main process of the proposed stratified SVM includes three main steps. First, we chose preliminary urban and non-urban training samples based on the values of the NTL, the NDVI, and the nighttime LST data; the urban seeds must both have a larger NTL and nighttime LST value than the average value and have a smaller NDVI value than the average value in the Chengdu area, and the non-urban seeds were selected in the opposite way. Second, based on the training seeds selected in the first step, we applied the stratified SVM classifier to other unknown pixels in an iterative method. Third, during the loop processing, the pixels identified as urban samples were placed into the next loop as new urban seeds, and the loop procedure was stopped until there were more newly assigned urban seeds.

3.3.4. Verification with Landsat-8 OLI Images and Statistics Data

Since an increasing amount of research employs finer resolution images to evaluate urban extraction results, Landsat-8 OLI data with a higher spatial resolution of 30 m were employed to illustrate the performance of the proposed urban extraction method. Since the

quality of Landsat-8 OLS data is often influenced by heavy clouds of bad weather, MODIS land cover data was employed to adjust the extraction results of cloud cover pixels. We first extracted the urban built-up area of Chengdu based on fine-resolution Landsat-8 data, then resampled the results to the same coarse resolution of 1000 m and compared these urban extraction results to evaluate the performance of the proposed method.

In detail, we used ENVI software to conduct a supervised classification method, namely, the Maximum Likelihood Estimation method, to extract the urban built-up area of Chengdu based on the Landsat-8 OLI data. Although the Landsat-8 OLI data have a finer resolution, the quality of the images may be affected by heavy clouds, especially the heavy clouds of subtropical monsoon humid climate in Chengdu. Therefore, we had to replace the value of some cloud-affected pixels with MODIS land cover data, which already classify the urban built-up area based on multiple remote sensing data sources.

3.3.5. SDE for the Direction of Built-Up Area Changes

According to related research [34–36], the SDE, which was proposed by Lefever, can reveal the spatial distribution characteristics of geographic elements [37]; the SDE can reflect the geographical spatial characteristics of urban economic elements, as well as their spatial and temporal distributions based on the center of gravity, the spatial distribution range and the direction and shape [38]. These geographic and urban economic elements include the urban built-up area, the vegetation coverage, and the other urban land-use types. In terms of the urban built-up area, the center of gravity of SDE can reflect the relative position of the built-up area change, and the azimuth of the SDE can represent the main direction of the urban development trend, while the long and short axis lengths can indicate the distribution of urban economic elements. In this research, the SDE was applied based on the urban built-up areas extracted by the proposed stratified SVM method; the details are described in the functions below.

To apply SDE, we first calculated the gravity center shown

$$(\bar{X}_w, \bar{Y}_w) = \left(\frac{\sum_{i=1}^n w_i x_i}{\sum_{i=1}^n w_i}, \frac{\sum_{i=1}^n w_i y_i}{\sum_{i=1}^n w_i} \right) \quad (1)$$

Then we calculated the SDE

$$SDE_x = \sqrt{\frac{\sum_{i=1}^n (x_i - \bar{x})^2}{n}} \quad (2)$$

$$SDE_y = \sqrt{\frac{\sum_{i=1}^n (y_i - \bar{y})^2}{n}} \quad (3)$$

Finally, we calculated the

$$\tan\theta = \frac{(\sum_{i=1}^n \tilde{x}_i^2 - \sum_{i=1}^n \tilde{y}_i^2) + \sqrt{(\sum_{i=1}^n \tilde{x}_i^2 - \sum_{i=1}^n \tilde{y}_i^2)^2 + 4(\sum_{i=1}^n \tilde{x}_i \tilde{y}_i)^2}}{2\sum_{i=1}^n \tilde{x}_i \tilde{y}_i} \quad (4)$$

Standard deviation of x -axis:

$$\sigma_x = \sqrt{2} \sqrt{\frac{\sum_{i=1}^n (\tilde{x}_i \cos\theta - \tilde{y}_i \sin\theta)^2}{n}} \quad (5)$$

Standard deviation of y -axis:

$$\sigma_y = \sqrt{2} \sqrt{\frac{\sum_{i=1}^n (\tilde{x}_i \sin\theta - \tilde{y}_i \cos\theta)^2}{n}} \quad (6)$$

In the Formulas 1-6, $Y(x_i, y_i)$ is the coordinate of each government in 20 areas in Chengdu; (\bar{X}, \bar{Y}) is the gravity center; n refers to the number of areas in Chengdu; w_i represents the weight of i th area; \tilde{x}_i and \tilde{y}_i is the deviation between coordinate and gravity center of the i th area.

3.3.6. Spatial Autocorrelation Analysis with Moran's I

As one of the spatial statistical analysis methods, spatial autocorrelation analysis can measure the correlation between a certain location and a neighboring location based on the same geographic features or geographic attribute values [34,36,38]. The global Moran's I index, which was introduced by Moran [31], can be employed to evaluate the spatial dependence of statistical geography in the neighboring location [34]. In addition, local Moran's I index can also be employed to reveal the characteristics of local spatial autocorrelation [34,36]. In terms of location spatial autocorrelation analysis, related research has commonly employed both Moran's scatter plots and spatially linked local indicators (LISA) [36], while the Moran's scatter plots can represent the spatial connection between research locations, and the LISA can indicate both the significance of the spatial connection and the difference between the research locations and neighboring locations. Therefore, global Moran's I index, local Moran's scatter plot and the LISA was adopted in this research to measure the spatial correlation of urban development in Chengdu from 2015 to 2019. The distribution of the values differs from -1 to 1 ; values ranging from 0 to 1 indicate that there is a positive correlation between geographical entities. There is a negative correlation between -1 and 0 , and there is no correlation if it equals 0 .

$$I = \frac{n}{\sum_{i=1}^n \sum_{j=1}^n w_{i,j}} * \frac{\sum_{i=1}^n \sum_{j=1}^n w_{i,j} (x_i - \tilde{x})(x_j - \tilde{x})}{\sum_{i=1}^n (x_i - \tilde{x})^2} \quad (7)$$

In the Formula (7), n means the number of the areas in Chengdu, x_i and x_j represent the expansion of urban built-up area in certain years from 2015 to 2019 in i area and j area, \tilde{x} is the mean value of the expansion of urban built-up area, $w_{i,j}$ is the spatial weight between i and j .

Furthermore, the social and economic census data could be employed to evaluate the extraction results of urban built-up areas. The GDP and population information were also used to illustrate the performance of the proposed method in Chengdu over the period 2015–2019. The correlation between the extracted urban built-up area and the GDP and the population was demonstrated to verify the extraction results of urban built-up areas.

4. Results

4.1. Urban Built-Up Area Changes in Chengdu (2015–2019)

Since the Landsat-8 OLI images have a 30 m spatial resolution, which is better than that of the NPP-VIIRS NTL data, the MODIS NDVI data, and the MODIS nighttime LST data, we employed the urban built-up area extract from Landsat-8 and MODIS Land Cover data as the reference data to evaluate the accuracy of the proposed urban extraction method. The overall accuracy (OA) and KAPPA values were employed to measure the performance of the proposed stratified SVM methods. Details of the evaluation results are listed in Table 1 below.

Table 1. The extraction accuracy.

Years	OA	KAPPA
2015	92.23%	0.6048
2016	93.17%	0.6561
2017	92.83%	0.6445
2018	92.69%	0.6519
2019	92.74%	0.6588

In Table 1, first, all the OA values are larger than 92% from 2015 to 2019, which illustrates the accuracy of the proposed method. Second, all the KAPPA values are more than 0.6, which can indicate the high correlation between the urban built-up area extracted by the proposed stratified SVM method and the urban built-up area extracted by Landsat-8 OLI and MODIS Land Cover data.

The confusion matrix of the urban built-up areas was extracted using the stratified SVM method from 2015 to 2019, as shown in Table 2. The urban built-up areas extracted from Landsat-8 OLI data and MODIS land cover data were used as the reference data and reprojected to 1000 m spatial resolution. A total of 14,259 sampling pixels were collected as validation data. The overall accuracy was larger than 92% from 2015 to 2019. After comparison with existing related research [16,25–27], the accuracy of the results could be accepted at the city level in Western China.

Table 2. The confusion matrix in Chengdu from 2015 to 2019.

		References Urban				
		2015	Urban areas	Non-urban areas	Row total	User's accuracy (%)
Extracted urban	Urban areas		1022	576	1598	63.95
	Non-urban areas		532	12,129	12,661	95.80
	Column total		1554	12,705	14,259	
Producer's accuracy (%)		65.77	95.47			OA = 92.23
		2016	Urban areas	Non-urban areas	Row total	User's accuracy (%)
Extracted urban	Urban areas		1107	517	1624	68.17
	Non-urban areas		457	12,178	12,635	96.38
	Column total		1564	12,695	14,259	
Producer's accuracy (%)		70.78	95.93			OA = 93.17
		2017	Urban areas	Non-urban areas	Row total	User's accuracy (%)
Extracted urban	Urban areas		1112	541	1653	67.27
	Non-urban areas		481	12,125	12,606	96.18
	Column total		1593	12,666	14,259	
Producer's accuracy (%)		69.81	95.73			OA = 92.83
		2018	Urban areas	Non-urban areas	Row total	User's accuracy (%)
Extracted urban	Urban areas		1178	558	1736	67.86
	Non-urban areas		485	12,038	12,523	98.28
	Column total		1663	12,596	14,259	
Producer's accuracy (%)		70.84	95.57			OA = 92.69
		2019	Urban areas	Non-urban areas	Row total	User's accuracy (%)
Extracted urban	Urban areas		1209	547	1756	68.85
	Non-urban areas		488	12,015	12,503	96.10
	Column total		1697	12,562	14,259	
Producer's accuracy (%)		71.24	95.65			OA = 92.74

In Table 2, the urban built-up area in Chengdu extracted using the stratified SVM method gradually increased from 1598 pixels in 2015 to 1756 pixels in 2019, which is consistent with the results in [16,25], which indicate that the urban built-up areas of Chengdu increased from 1992 to 2012.

Furthermore, the details of urban extraction results from 2015 to 2019 are listed in Figure 4 below.

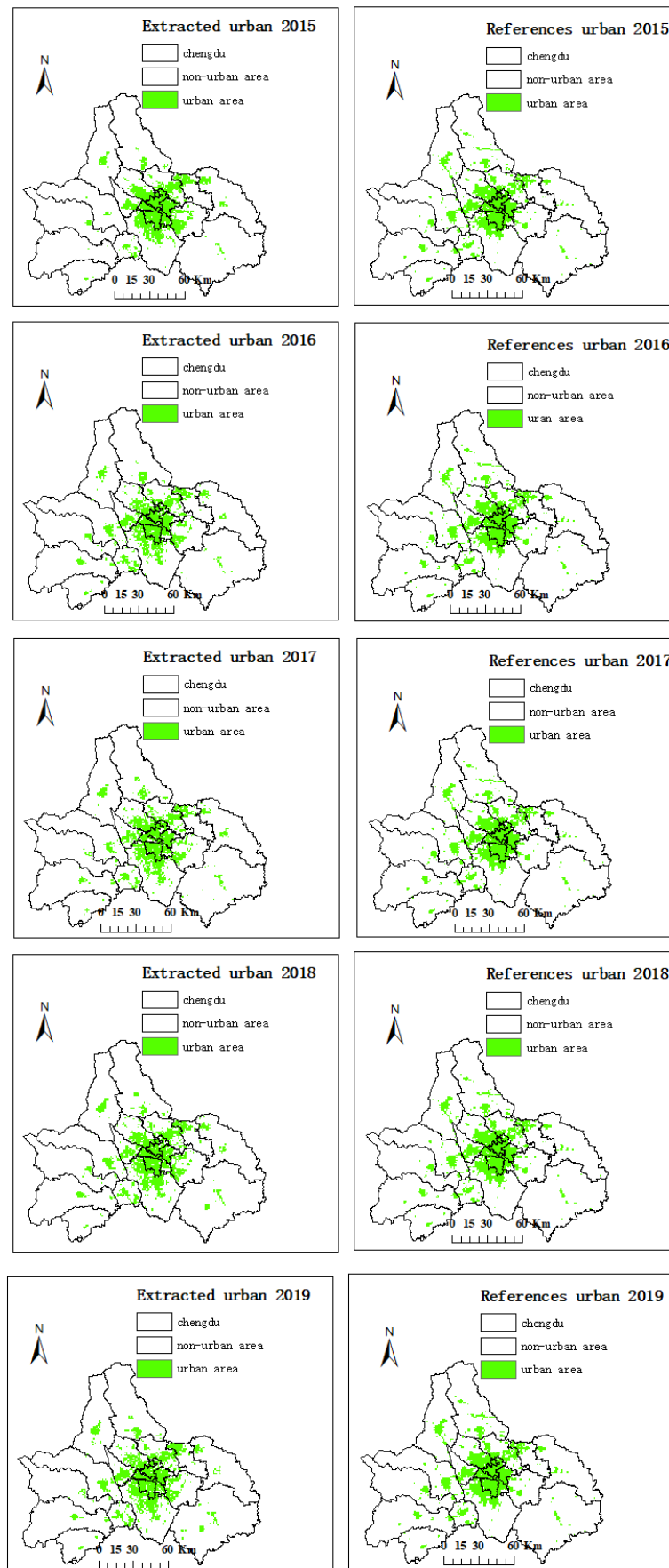


Figure 4. Urban built-up area change of Chengdu.

As illustrated in Figure 4, the green pixels increased gradually from 2015 to 2019, which clearly reflects the stable urban built-up area increases over the five years; to better represent the development of the urban built-up area, we combine the change of the extracted urban built-up area of the five years into a single graph, as shown in Figure 5 below.

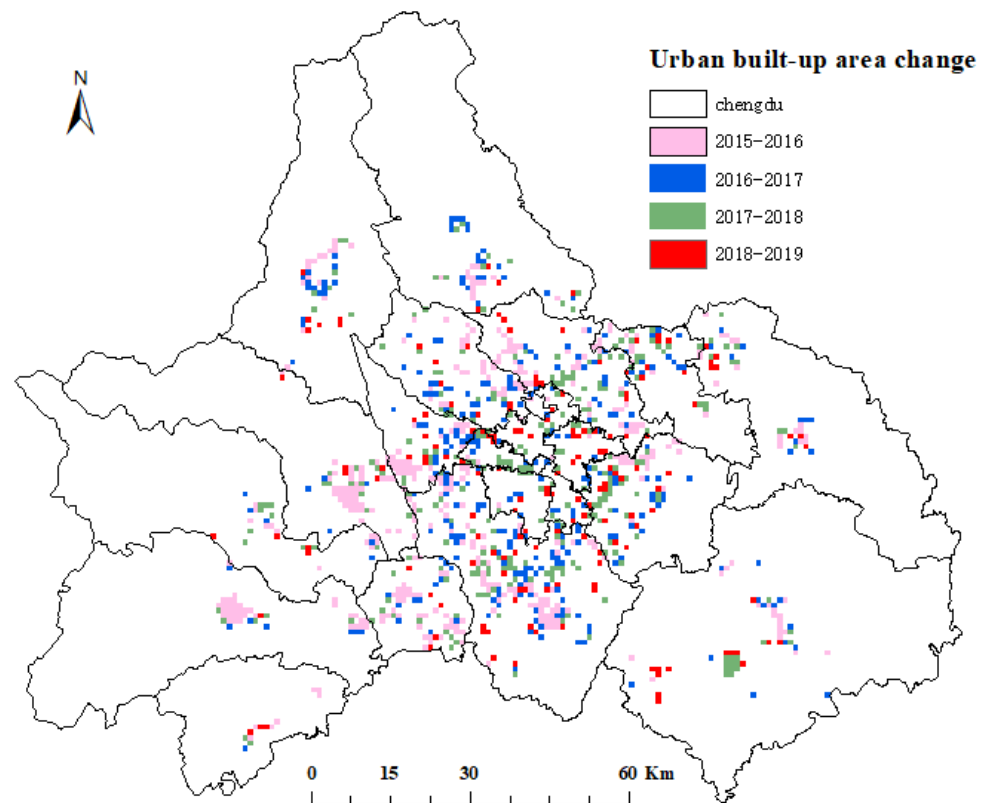


Figure 5. Change of extracted urban built-up areas in Chengdu.

As demonstrated in Figure 5, four different colors indicate the change of extracted urban built-up areas in Chengdu from 2015 to 2019. The pink color pixels, the blue color pixel, the green color pixels, and the red color pixels represent the urban built-up area increase during 2015–2016, 2016–2017, 2017–2018, and 2018–2019, respectively. This can also demonstrate the growth of the urban built-up area in Chengdu during these five years.

4.2. Direction of Urban Built-Up Area Changes in Chengdu (2015–2019)

According to the urban built-up area extraction results, the distribution of these urban built-up areas is extremely unbalanced, for instance, most urban built-up areas are concentrated in Jinjiang, Qingyang, Jinniu, Wuhou, and Chenghua districts; meanwhile, other districts have relatively fewer urban built-up area. This unbalanced distribution of extracted urban built-up areas illustrates the uneven development of different districts in Chengdu over the five years.

In terms of specific urban built-up areas in 20 different districts in Chengdu, the extracted urban built-up areas are listed in Figure 6 below. All the extracted urban built-up areas of different districts in Chengdu increased stably from 2015 to 2019. However, some districts increased slowly, while other districts increased quickly, for instance, the urban built-up area in Xindu, Shuangliu and Pidu districts grew faster than other districts in Chengdu over the five years. These unbalanced growth of the urban built-up area in different districts can also clearly demonstrate the uneven development between different districts in Chengdu over the five years.

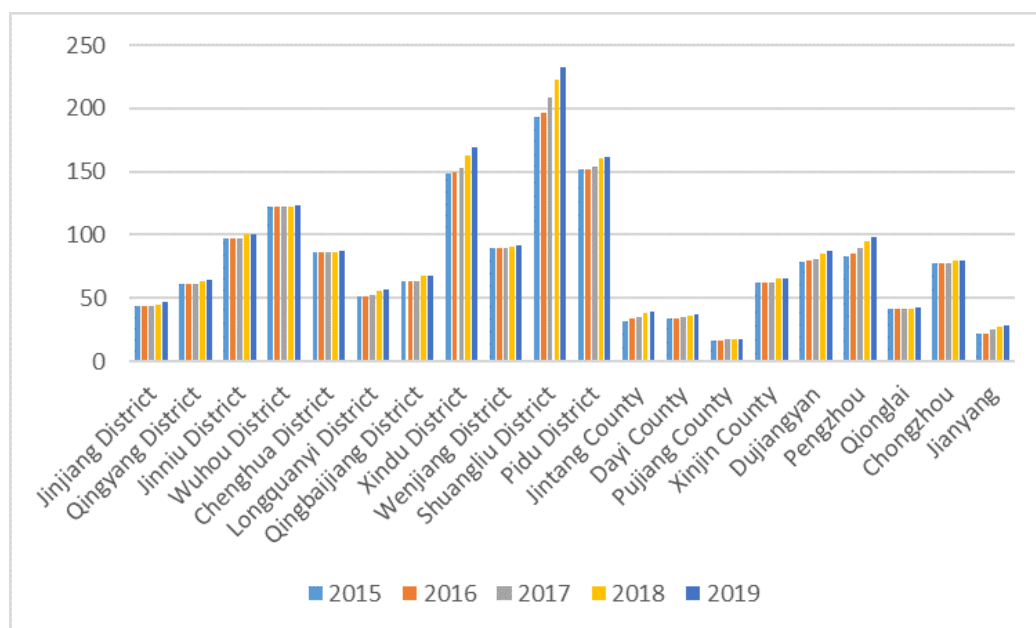


Figure 6. Extracted urban built-up area in different districts in Chengdu.

To further analyze the pattern of urban built-up areas in Chengdu over the period 2015–2019, the SDE method was employed to explore the spatial distribution and evolution pattern of urban growth in Chengdu from 2015 to 2019. The details of the SDE method are listed in Table 3, Figures 7 and 8, respectively, as below.

Table 3. Standard Deviation Ellipse data of the urban built-up area in Chengdu.

Years	Center Coordinates	Length of Long Axis (km)	Length of Short Axis (km)	Area of the Ellipse (km ²)
2015	(103.57 E, 30.42 N)	44.75	36.99	5200
2016	(103.58 E, 30.42 N)	45.09	37.19	5268
2017	(103.58 E, 30.42 N)	45.97	37.75	5450
2018	(103.58 E, 30.41 N)	46.22	38.11	5533
2019	(103.58 E, 30.41 N)	47.24	38.03	5643

The results of SDE analysis indicate that the spatial evolution of built-up area change in Chengdu over the period 2015–2019 demonstrated a “northwest-southeast” spatial expansion pattern. Over the five years, the change in the length of the long axis was greater than that of the length of the short axis, which indicated that the stronger urban extension trends followed the north to south direction. The length of the long axis, the length of the short axis, and the area of the SDE ellipse gradually increased from 2015 to 2019, which correlates with the stable growth of the extracted urban built-up areas in Chengdu. The increase in SDE ellipse was relatively slower from 2015 to 2016 than that from 2017 to 2019, which also corresponds with the socioeconomic census data.

Considering the gravity change in the urban built-up area in Chengdu from 2015 to 2019, as illustrated in Figure 8, all the centers of gravity of urban built-up areas were located in Qingyang district over the five years. In detail, the evolution of the center of gravity mainly followed the north to south direction, and only the center of gravity deviated to the southwest to some extent in 2018, which also reflects the socioeconomic census data over the five years in Chengdu. In addition, the change distance of the center of gravity in 2018 and 2019 was greater than that from 2015 to 2017, which reflected the faster urbanization in 2018 and 2019 in Chengdu.

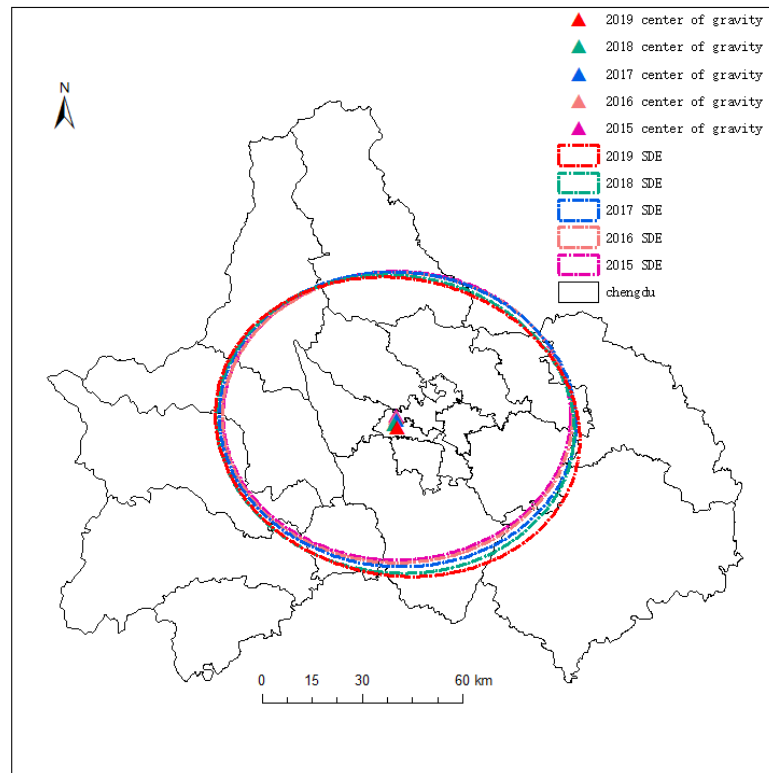


Figure 7. Standard Deviation Ellipse data of the urban built-up area in Chengdu.

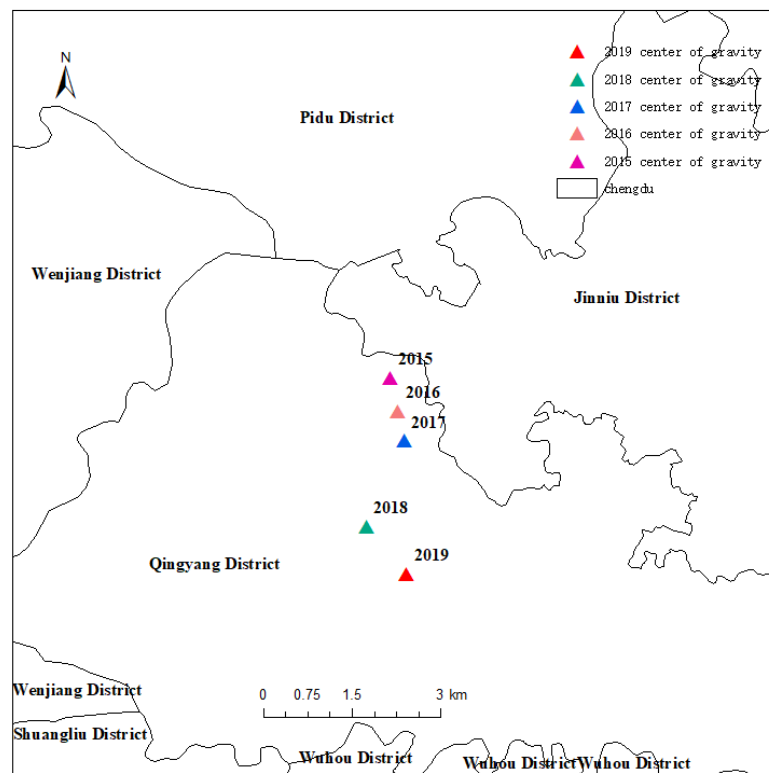


Figure 8. Center of gravity of urban built-up area in Chengdu.

4.3. Relations between the Spatial Variations in Chengdu

In order to further explore the built-up area change pattern in Chengdu, the spatial autocorrelation analysis method was also employed to study the spatial autocorrelation pattern from 2015 to 2019. In detail, global Moran's I index, the local Moran's scatter plot and the spatial local indication of spatial association (LISA) cluster map were employed to unveil the spatial autocorrelation pattern of the urban extension from 2015 to 2019. In addition, the calculated results are demonstrated in Table 4 and Figure 9 as follows. As presented in Table 4, all the p values were significantly lower than 0.001, which not only proves that global Moran's I index passed the significance test, but also shows that the urban evolution in Chengdu from 2015 to 2019 was clustered. In addition, global Moran's I indexes were all positive and larger than 0.5, which clearly illustrates a high spatial correlation. Although both the global Moran's I index value and the z value decreased from 2015 to 2017, both of them increased and were larger than those in 2015, which can demonstrate that the overall spatial correlation became stronger with urban spatial extension, even with fluctuations in some years. Local Moran's scatter plot and the LISA cluster map were adopted to further investigate the local spatial correlation in 20 different districts in Chengdu from 2015 to 2019; the details are listed in Figure 9.

Table 4. Global Moran's I index.

Years	Global Moran's I Index	z Value	p Value
2015	0.530	4.001	<0.001
2016	0.529	3.997	<0.001
2017	0.523	3.947	<0.001
2018	0.538	4.078	<0.001
2019	0.544	4.113	<0.001

The local Moran's scatter plot changed from 2015 to 2019, which reflects the change in local spatial correlations in Chengdu. From 2015 to 2017, the slope of the local Moran's scatter plot line decreased as the Moran's I value decreased from 0.530 to 0.523, which shows that the spatial correlation reduced with the built-up area change in these years. However, the slope of the local Moran's scatter plot line increased from 2018 to 2019 and was larger than that in 2015, which demonstrates that the spatial correlation became stronger with the urban extension from 2018 to 2019. In addition, the LISA cluster map was the same from 2015 to 2019, which showed a stable cluster pattern among different districts in Chengdu over the five years. The "High-High" clusters, which include six districts, namely, Jinjiang, Qingyang, Jinniu, Wuhou, Chenghua and Shuangliu districts, are located in the central and south parts of Chengdu. These districts all have relatively larger urban built-up areas, a greater population and a higher GDP than other districts in Chengdu. Meanwhile, the "Low-Low" cluster, which includes two districts, namely, Qionglai and Dayi districts, is located in the west parts of Chengdu; these two districts are relatively slower in urbanization, with smaller urban built-up areas, a lower population, and a lower GDP than other districts in Chengdu.

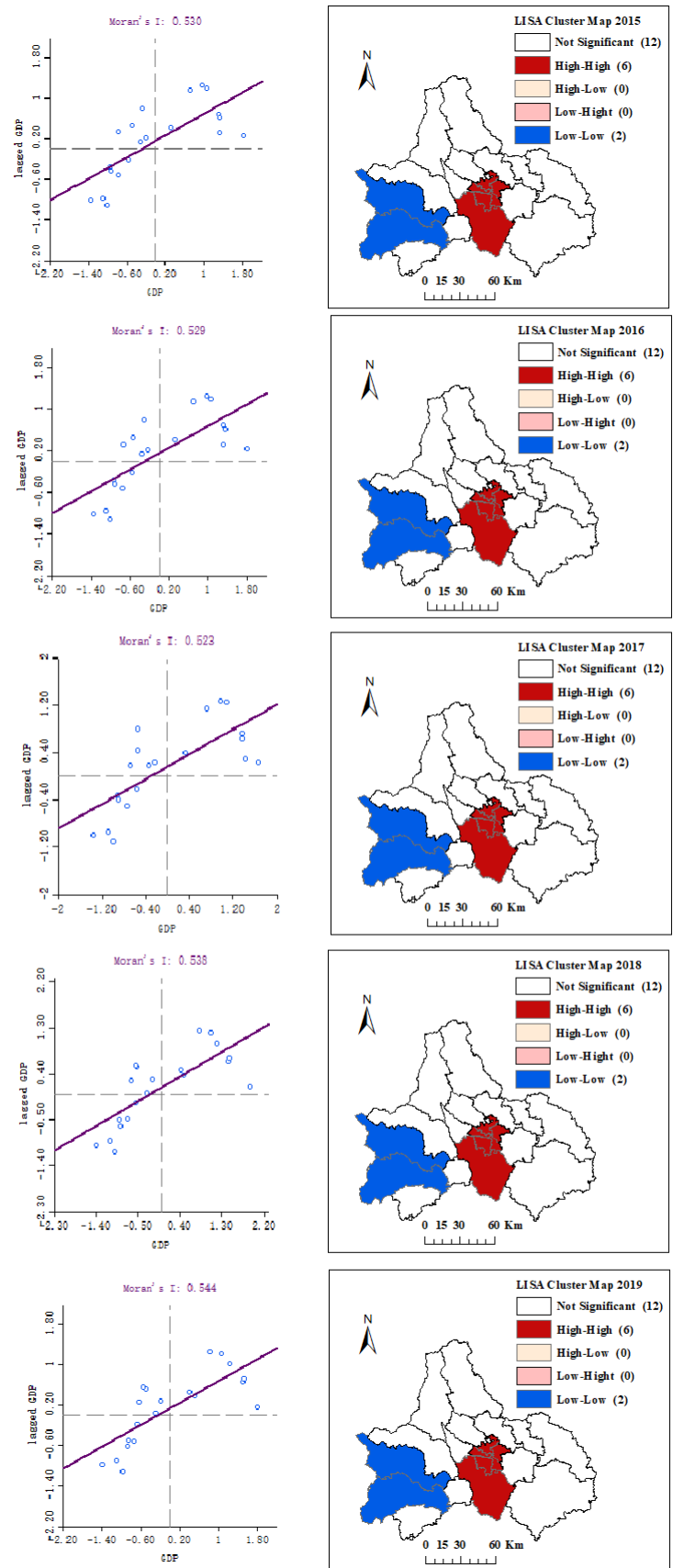


Figure 9. Local Moran's scatter plot and LISA cluster map.

5. Discussion

5.1. Significance of The Study

The NPP-VIIRS NTL data, which has higher quality than DMSP/OLS NTL data, is used in this research to measure the urban built-up area change in Chengdu from 2015 to 2019, the extracted results obtained by the stratified SVM method are consistent with the urban built-up area extraction results in [16], which demonstrate the urban land increase from 889 km² with an average annual increase percentage of 19.83% from 1992 to 2012. Furthermore, these extraction results are also in accordance with the global annual urban dynamics obtained from the DMSP/OLS from 1992 to 2013 [39]; their results indicate the fast urbanization process in developing countries in Asia [40], South America [41], and Africa [42] contribute most growth of urban built-up areas in the world. This can illustrate the values of the NTL data to continually monitor the spatial-temporal urban dynamics globally during a long period. These evaluation results indicate the freely accessed NTL data can be employed as a promising auxiliary approach to the expensive and time-consuming surveys and field experiments in urban studies, especially for the underdeveloped western cities with tight budgets in China. Moreover, the socioeconomic validation results illustrate the high correlation between the urban built-up areas, the GDP, and the urban population.

In addition to the built-up area change in Chengdu from 2015 to 2019, the spatial-temporal urban evaluation pattern and the geographic correlation were also investigated in this research. The results of the SDE analysis indicate that the spatial evolution of built-up area change in Chengdu over the period 2015–2019 demonstrated a “northwest-southeast” spatial expansion pattern. Over the five years, the change in the length of the long axis was greater than that of the length of the short axis, which indicates the stronger built-up area change trend that follows the north to south direction. In addition, the center of gravity also mainly followed the north to south directions, with the exception that the center of gravity deviated to the southwest to some extent in 2018. These SDE analysis results are in accordance with the results in [17], which indicate that the built-up area change direction in Chengdu was mainly toward the northwest, west, and southwest from 1978 to 2010.

Furthermore, the results of Global and Local Moran’s *I* index analysis in Chengdu from 2015 to 2019 indicate the significant “High-High” and “Low-Low” cluster, which demonstrates that the strong districts with higher GDP tightly correlate with strong districts, while poor districts with lower GDP collaborate closely with poor districts in Chengdu, which can demonstrate the impact of power on uneven development in Chengdu from 2015 to 2019.

5.2. Relationship of the Result and Other Indexes of Uneven Development

To illustrate the relationship between the urban built-up areas and the statistics data. We further separated the growth of different districts and counties, as shown in Figure 10, in which the larger size of the blue pie chart, the faster the growth.

In Figure 10, we can conclude that there was strong economic development momentum in the eastern and western parts where the size of the blue pie chart is the largest. Conversely, slow economic development was witnessed in the northern and southern parts. The central part, which is also the urban district, experienced stable economic development. Considering the trend of the city center to move southward and eastward, the south and east parts actually consumed more rural land to generate similar GDP growth.

According to related research [16,25,27], socioeconomic census data were also employed to evaluate the accuracy of the extracted urban built-up area over the period 2015–2019 in Chengdu. In detail, the correlation between the extracted urban built-up area and the GDP and the urban population is demonstrated in Figure 11. The relationships between the extracted urban built-up areas, the GDP, and the Population in Chengdu from 2015 to 2019 are discussed; the results demonstrate that the extracted urban built-up areas were highly correlated with the GDP throughout the five years, which clearly shows the accuracy of the proposed urban extraction method. Similarly, the correlation between

urban built-up areas and the urban population was calculated in Chengdu from 2015 to 2019; the results illustrate that the extracted urban built-up areas had a strong correlation with the urban population, which also clearly indicates the performance of the proposed research method.

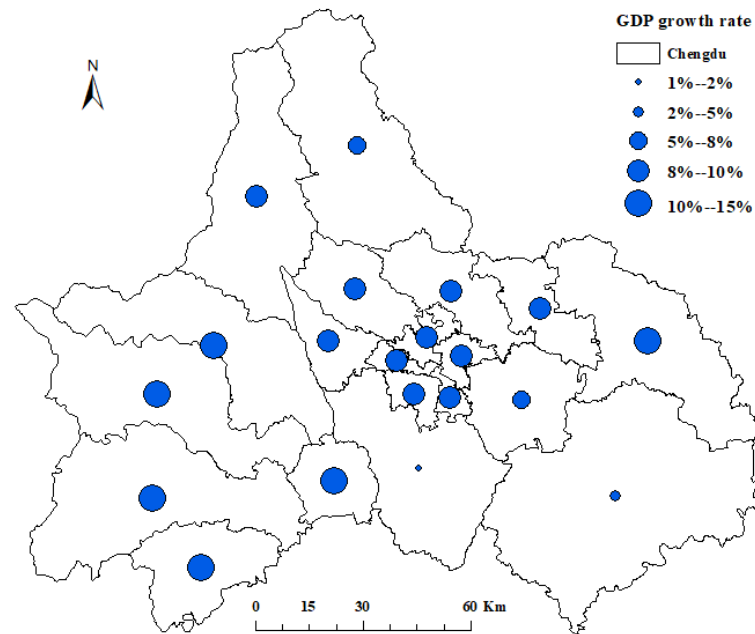


Figure 10. The quantitative analysis of GDP growth rate from 2015 to 2019.

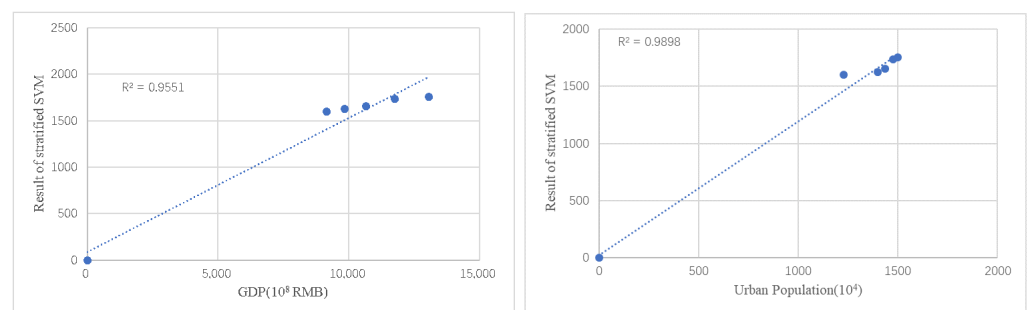


Figure 11. The correlation between built-up area and GDP/urban population.

In terms of [43], uneven development is not only reflected by urban built-up areas, but also represented in other fields, such as investment and urban population. Therefore, this research tries to visualize the changing pattern of GDP and urban population, and compares it with the evolution pattern of urban built-up areas. The evaluation results illustrate the same evolution pattern between built-up areas, the GDP, and the urban population. This can also prove the uneven development in Chengdu during these five years. Furthermore, how to design a scientific spatial-temporal monitoring system with multiple parameters of uneven development is vital for future studies.

5.3. Limitations and Future Research

There are some limitations in this research that must be addressed in future research. For example, the urban extraction in this research was mainly based on the NPP-VIIRS NTL data, the NDVI data and the nighttime LST data; their spatial resolution may not have been high enough for the complex urban scenario. Recently, some research has already tried to extract urban built-up areas based on the high-resolution Landsat data [44].

Therefore, future research should be based on remote sensing information with higher spatial resolution. Furthermore, since the quality of remote sensing images is highly vulnerable due to the clouds and weather conditions, the weather in Chengdu, like a typical city in Western China, may constrain the performance of remote sensing methods; therefore, more field experiments for urban coverage and urban land use in urban built-up areas are also required in future related studies to improve the accuracy of the urban built-up area change.

6. Conclusions

Complex human behaviors dramatically affect the urban environment and urban land exploitation; therefore, a timely and accurate understanding of the spatial-temporal expansion pattern of cities is crucial for better urban living and sustainable urban development. The spatial-temporal urban development characteristics of Chengdu over the period 2015–2019 were explored in this paper. The extension of urban built-up area, the spatial evolution of built-up area change and the geographic spatial correlation within Chengdu were investigated. The results demonstrated in this research could supply useful references and guidance for urban land use and urban management in western cities.

This research tried to measure the built-up area change pattern, especially the spatial evaluation pattern of urban built-up area change and the geographic spatial correlation pattern, in Chengdu from 2015 to 2019. A stratified SVM method for the urban built-up area extraction method was presented. Remote sensing information, mainly including the NTL data, the NDVI data, and the nighttime LST data, was employed to extract the urban built-up area. Based on the SDE and Moran's index analysis, the built-up area change pattern, the spatial evaluation pattern and the spatial correlation pattern were discussed.

The timely and accurate measurement of the spatial-temporal pattern of urban evolution is vital for urban construction and planning, especially for underdeveloped western cities in China. The scientific measurement and understanding of the built-up area change pattern are crucial for efficient land usage decisions and urban management planning.

Author Contributions: Conceptualization, L.L., Z.L. (Zehao Li) and X.L.; methodology, Z.L. (Zehao Li); software, X.F.; validation, L.L., X.L. and W.Z.; formal analysis, Z.L. (Zhichao Li) and W.Z.; writing—original draft preparation, L.L. and X.L.; writing—review and editing, X.L. and W.Z.; visualization, Z.L. (Zhichao Li); funding acquisition, L.L., X.L., Z.L. (Zehao Li) and W.Z. All authors have read and agreed to the published version of the manuscript.

Funding: This work was funded by the Ministry of Education through the Humanities and Social Science project [Grant No. 19YJC630104]; the UESTC Funds for Important Social Science Research [Grant No. 2021FRJHZD003]; and the National Natural Science Foundation of China [Grant No. 71974057, and Grant No. 72071031].

Institutional Review Board Statement: Not applicable.

Informed Consent Statement: Not applicable.

Data Availability Statement: Not applicable.

Conflicts of Interest: The authors declare no conflict of interest.

References

1. Harvey, D. *Social Justice and the City*; University of Georgia Press: Athens, GA, USA, 2010; Volume 1.
2. Smith, N. Toward a theory of gentrification a back to the city movement by capital, not people. *J. Am. Plan. Assoc.* **1979**, *45*, 538–548. [[CrossRef](#)]
3. Lin, G.C. Chinese urbanism in question: State, society, and the reproduction of urban spaces. *Urban Geogr.* **2007**, *28*, 7–29. [[CrossRef](#)]
4. Ye, C.; Chen, M.; Chen, R.; Guo, Z. Multi-scalar separations: Land use and production of space in Xianlin, a university town in Nanjing, China. *Habitat Int.* **2014**, *42*, 264–272. [[CrossRef](#)]
5. Li, Z.; Li, X.; Wang, L. Speculative urbanism and the making of university towns in China: A case of Guangzhou University Town. *Habitat Int.* **2014**, *44*, 422–431. [[CrossRef](#)]

6. Yeung, H.W.c. Rethinking mechanism and process in the geographical analysis of uneven development. *Dialogues Hum. Geogr.* **2019**, *9*, 226–255. [[CrossRef](#)]
7. Elvidge, C.D.; Zhizhin, M.; Ghosh, T.; Hsu, F.C.; Taneja, J. Annual time series of global VIIRS nighttime lights derived from monthly averages: 2012 to 2019. *Remote Sens.* **2021**, *13*, 922. [[CrossRef](#)]
8. Zheng, Y.; He, Y.; Zhou, Q.; Wang, H. Quantitative Evaluation of Urban Expansion using NPP-VIIRS Nighttime Light and Landsat Spectral Data. *Sustain. Cities Soc.* **2022**, *76*, 103338. [[CrossRef](#)]
9. Gao, K.; Yuan, Y. Spatiotemporal pattern assessment of China's industrial green productivity and its spatial drivers: Evidence from city-level data over 2000–2017. *Appl. Energy* **2022**, *307*, 118248. [[CrossRef](#)]
10. Jiang, L.; Liu, Y.; Wu, S.; Yang, C. Study on Urban Spatial Pattern Based on DMSP/OLS and NPP/VIIIRS in Democratic People's Republic of Korea. *Remote Sens.* **2021**, *13*, 4879. [[CrossRef](#)]
11. You, H.; Yang, J.; Xue, B.; Xiao, X.; Xia, J.; Jin, C.; Li, X. Spatial evolution of population change in Northeast China during 1992–2018. *Sci. Total Environ.* **2021**, *776*, 146023. [[CrossRef](#)]
12. Yu, M.; Guo, S.; Guan, Y.; Cai, D.; Zhang, C.; Fraedrich, K.; Liao, Z.; Zhang, X.; Tian, Z. Spatiotemporal Heterogeneity Analysis of Yangtze River Delta Urban Agglomeration: Evidence from Nighttime Light Data (2001–2019). *Remote Sens.* **2021**, *13*, 1235. [[CrossRef](#)]
13. Zheng, Y.; Tang, L.; Wang, H. An improved approach for monitoring urban built-up areas by combining NPP-VIIRS nighttime light, NDVI, NDWI, and NDBI. *J. Clean. Prod.* **2021**, *328*, 129488. [[CrossRef](#)]
14. Zhou, Y.; Li, C.; Zheng, W.; Rong, Y.; Liu, W. Identification of urban shrinkage using NPP-VIIRS nighttime light data at the county level in China. *Cities* **2021**, *118*, 103373. [[CrossRef](#)]
15. Ma, T.; Zhou, Y.; Zhou, C.; Haynie, S.; Pei, T.; Xu, T. Night-time light derived estimation of spatio-temporal characteristics of urbanization dynamics using DMSP/OLS satellite data. *Remote Sens. Environ.* **2015**, *158*, 453–464. [[CrossRef](#)]
16. He, C.; Liu, Z.; Tian, J.; Ma, Q. Urban expansion dynamics and natural habitat loss in China: A multiscale landscape perspective. *Glob. Chang. Biol.* **2014**, *20*, 2886–2902. [[CrossRef](#)] [[PubMed](#)]
17. Peng, W.; Wang, G.; Zhou, J.; Zhao, J.; Yang, C. Studies on the temporal and spatial variations of urban expansion in Chengdu, western China, from 1978 to 2010. *Sustain. Cities Soc.* **2015**, *17*, 141–150. [[CrossRef](#)]
18. Ma, L.; Wu, J.; Li, W.; Peng, J.; Liu, H. Evaluating saturation correction methods for DMSP/OLS nighttime light data: A case study from China's cities. *Remote Sens.* **2014**, *6*, 9853–9872. [[CrossRef](#)]
19. Xiao, P.; Wang, X.; Feng, X.; Zhang, X.; Yang, Y. Detecting China's urban expansion over the past three decades using nighttime light data. *IEEE J. Sel. Top. Appl. Earth Obs. Remote Sens.* **2014**, *7*, 4095–4106. [[CrossRef](#)]
20. Wei, Y.; Liu, H.; Song, W.; Yu, B.; Xiu, C. Normalization of time series DMSP-OLS nighttime light images for urban growth analysis with pseudo invariant features. *Landsc. Urban Plan.* **2014**, *128*, 1–13. [[CrossRef](#)]
21. Elvidge, C.D.; Baugh, K.E.; Zhizhin, M.; Hsu, F.C. Why VIIRS data are superior to DMSP for mapping nighttime lights. *Proc. Asia-Pac. Adv. Netw.* **2013**, *35*, 62. [[CrossRef](#)]
22. Shi, K.; Yu, B.; Huang, Y.; Hu, Y.; Yin, B.; Chen, Z.; Chen, L.; Wu, J. Evaluating the ability of NPP-VIIRS nighttime light data to estimate the gross domestic product and the electric power consumption of China at multiple scales: A comparison with DMSP-OLS data. *Remote Sens.* **2014**, *6*, 1705–1724. [[CrossRef](#)]
23. Xie, Y.; Weng, Q.; Weng, A. A comparative study of NPP-VIIRS and DMSP-OLS nighttime light imagery for derivation of urban demographic metrics. In Proceedings of the 2014 Third International Workshop on Earth Observation and Remote Sensing Applications (EORSA), Changsha, China, 11–14 June 2014; pp. 335–339.
24. Dou, Y.; Liu, Z.; He, C.; Yue, H. Urban land extraction using VIIRS nighttime light data: An evaluation of three popular methods. *Remote Sens.* **2017**, *9*, 175. [[CrossRef](#)]
25. Xu, M.; He, C.; Liu, Z.; Dou, Y. How did urban land expand in China between 1992 and 2015? A multi-scale landscape analysis. *PLoS ONE* **2016**, *11*, e0154839. [[CrossRef](#)]
26. Cao, X.; Chen, J.; Imura, H.; Higashi, O. A SVM-based method to extract urban areas from DMSP-OLS and SPOT VGT data. *Remote Sens. Environ.* **2009**, *113*, 2205–2209. [[CrossRef](#)]
27. Yang, Y.; He, C.; Zhang, Q.; Han, L.; Du, S. Timely and accurate national-scale mapping of urban land in China using Defense Meteorological Satellite Program's Operational Linescan System nighttime stable light data. *J. Appl. Remote Sens.* **2013**, *7*, 073535. [[CrossRef](#)]
28. Vapnik, V. *The Nature of Statistical Learning Theory*; Springer Science & Business Media: Springer: Cham, Switzerland, 1999.
29. Lu, C.; Li, L.; Lei, Y.; Ren, C.; Su, Y.; Huang, Y.; Chen, Y.; Lei, S.; Fu, W. Coupling Coordination Relationship between Urban Sprawl and Urbanization Quality in the West Taiwan Strait Urban Agglomeration, China: Observation and Analysis from DMSP/OLS Nighttime Light Imagery and Panel Data. *Remote Sens.* **2020**, *12*, 3217. [[CrossRef](#)]
30. Wang, X.; Cong, P.; Jin, Y.; Jia, X.; Wang, J.; Han, Y. Assessing the Effects of Land Cover Land Use Change on Precipitation Dynamics in Guangdong–Hong Kong–Macao Greater Bay Area from 2001 to 2019. *Remote Sens.* **2021**, *13*, 1135. [[CrossRef](#)]
31. Moran, P.A. The interpretation of statistical maps. *J. R. Stat. Soc. Ser. B (Methodol.)* **1948**, *10*, 243–251. [[CrossRef](#)]
32. Sulla-Menashe, D.; Gray, J.M.; Abercrombie, S.P.; Friedl, M.A. Hierarchical mapping of annual global land cover 2001 to present: The MODIS Collection 6 Land Cover product. *Remote Sens. Environ.* **2019**, *222*, 183–194. [[CrossRef](#)]
33. Yang, Y.; Xiao, P.; Feng, X.; Li, H. Accuracy assessment of seven global land cover datasets over China. *ISPRS J. Photogramm. Remote Sens.* **2017**, *125*, 156–173. [[CrossRef](#)]

34. Zhong, Y.; Lin, A.; He, L.; Zhou, Z.; Yuan, M. Spatiotemporal dynamics and driving forces of urban land-use expansion: A case study of the Yangtze River economic belt, China. *Remote Sens.* **2020**, *12*, 287. [[CrossRef](#)]
35. Guo, L.; Gong, H.; Ke, Y.; Zhu, L.; Li, X.; Lyu, M.; Zhang, K. Mechanism of Land Subsidence Mutation in Beijing Plain under the Background of Urban Expansion. *Remote Sens.* **2021**, *13*, 3086. [[CrossRef](#)]
36. Zhong, Y.; Lin, A.; Xiao, C.; Zhou, Z. Research on the Spatio-Temporal Dynamic Evolution Characteristics and Influencing Factors of Electrical Power Consumption in Three Urban Agglomerations of Yangtze River Economic Belt, China Based on DMSP/OLS Night Light Data. *Remote Sens.* **2021**, *13*, 1150. [[CrossRef](#)]
37. Lefever, D.W. Measuring geographic concentration by means of the standard deviational ellipse. *Am. J. Sociol.* **1926**, *32*, 88–94. [[CrossRef](#)]
38. Yuan, J.; Bian, Z.; Yan, Q.; Gu, Z.; Yu, H. An approach to the temporal and spatial characteristics of vegetation in the growing season in Western China. *Remote Sens.* **2020**, *12*, 945. [[CrossRef](#)]
39. Zhou, Y.; Li, X.; Asrar, G.R.; Smith, S.J.; Imhoff, M. A global record of annual urban dynamics (1992–2013) from nighttime lights. *Remote Sens. Environ.* **2018**, *219*, 206–220. [[CrossRef](#)]
40. Zhou, N.; Hubacek, K.; Roberts, M. Analysis of spatial patterns of urban growth across South Asia using DMSP-OLS nighttime lights data. *Appl. Geogr.* **2015**, *63*, 292–303. [[CrossRef](#)]
41. Andrade-Núñez, M.J.; Aide, T.M. Built-up expansion between 2001 and 2011 in South America continues well beyond the cities. *Environ. Res. Lett.* **2018**, *13*, 084006. [[CrossRef](#)]
42. Jiang, S.; Wei, G.; Zhang, Z.; Wang, Y.; Xu, M.; Wang, Q.; Das, P.; Liu, B. Detecting the Dynamics of Urban Growth in Africa Using DMSP/OLS Nighttime Light Data. *Land* **2020**, *10*, 13. [[CrossRef](#)]
43. Ye, C.; Chen, M.; Duan, J.; Yang, D. Uneven development, urbanization and production of space in the middle-scale region based on the case of Jiangsu province, China. *Habitat Int.* **2017**, *66*, 106–116. [[CrossRef](#)]
44. Liu, X.; Huang, Y.; Xu, X.; Li, X.; Li, X.; Ciais, P.; Lin, P.; Gong, K.; Ziegler, A.D.; Chen, A.; et al. High-spatiotemporal-resolution mapping of global urban change from 1985 to 2015. *Nat. Sustain.* **2020**, *3*, 564–570. [[CrossRef](#)]